Lawrence Berkeley Laboratory
UNIVERSITY OF CALIFORNIA

Materials & Molecular Research Division

Submitted to Engineering Fracture Mechanics

PREDICTION OF LOW-CYCLE FATIGUE-LIFE BY ACOUSTIC EMISSION
PART 1: 2024-T3 ALUMINUM ALLOY
PART 2: ALCLAD 7075-T6/ALUMINUM ALLOY

J. Baram and M. Rosen

May 1980

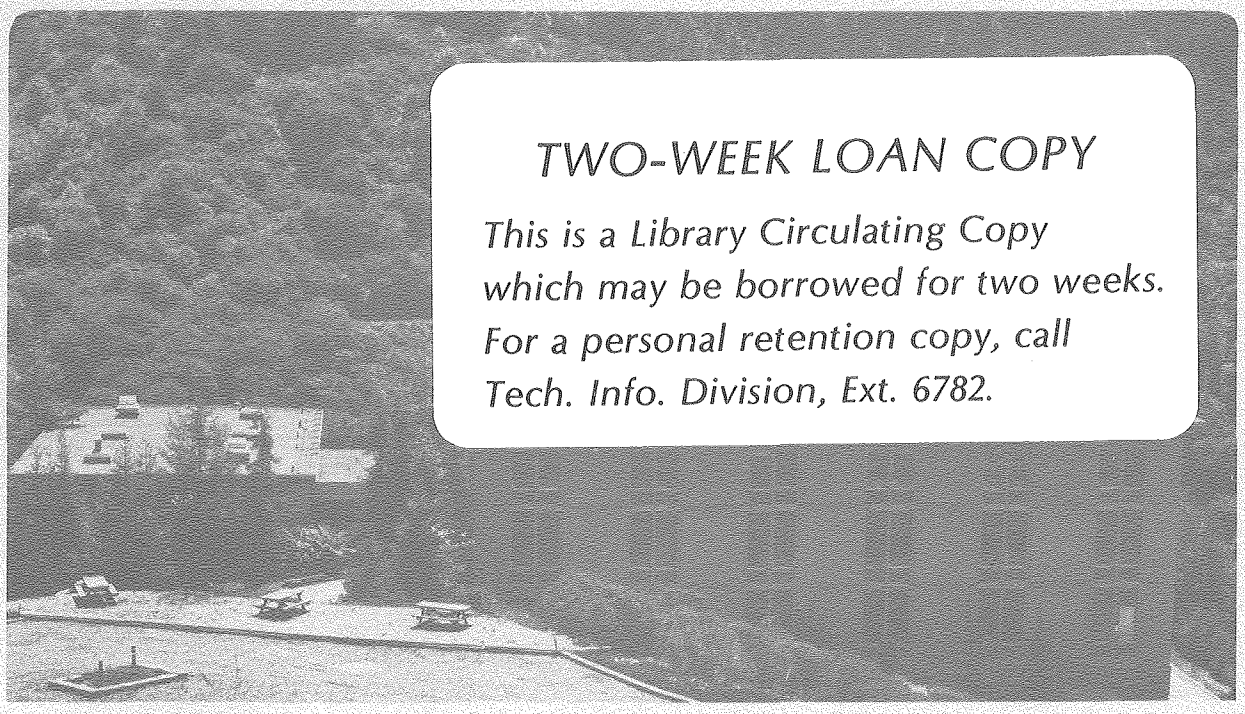

Prepared for the U.S. Department of Energy under Contract W-7405-ENG-48

DISCLAIMER

PREDICTION OF LOW-CYCLE FATIGUE-LIFE BY ACOUSTIC EMISSION
PART 1: 2024-T3 ALUMINUM ALLOY

J. Baram
Materials Engineering Division
Ben-Gurion University of the Negev
Beer-Sheva, Israel

and

M. Rosen*
Materials and Molecular Research Division
Lawrence Berkeley Laboratory, University of California
Berkeley, California 94720

ABSTRACT

Low-cycle fatigue tests were conducted by tension-compression until rupture, on a 2024-T3 aluminum alloy sheet. Initial crack sizes and orientations in the fatigue specimens were found to be randomly distributed. Acoustic emission was continuously monitored during the tests. Every few hundred cycles, the acoustic signal having the highest peak-amplitude, was recorded as an extremal event for the elapsed period. This high peak-amplitude is related to a fast crack propagation rate through a phenomenological relationship. The extremal peak-amplitudes are shown by an ordered statistics treatment, to be extremally distributed. The statistical treatment enables the prediction of the number of cycles left until failure. Predictions performed a-posteriori based on results gained early in each fatigue test are in good agreement with actual fatigue lives. The amplitude distribution analysis of the acoustic signals emitted during cyclic stress appears to be a promising nondestructive method of predicting fatigue life.

---

*On leave from the Materials Engineering Department, Ben-Gurion University, Beer-Sheva, Israel.

INTRODUCTION

There is a continuously increasing interest in monitoring and predicting fatigue crack-growth in order to prevent catastrophic failures and to assess the reliability of components and structures in a realistic manner. Recently the aircraft, automobile and nuclear industries have developed much concern, and invested much effort, in fatigue crack-propagation studies for reasons of safety and economy. Review papers have been lately published on fatigue crack-growth prediction methods [1-3]. Many crack propagation laws have been proposed and compared with experimental results [4]. Data are generally obtained by conducting experiments, with appropriately designed pre-notched specimens. Performing nondestructive monitoring on fatigue-loaded structures or components during service in order to predict the time until fatigue is yet a challenge to be met.

The advent of acoustic emission techniques holds promise of providing such a monitoring tool. Acoustic emission is generated by the abrupt redistribution of stresses in the vicinity of a defect. The strain energy is emitted as an elastic wave, whose surface components (Lamb or Rayleigh waves) are detected and analyzed. These particular wave propagation modes have geometrical losses as R^{-1}, where R is the distance from the source (as opposed to R^{-2}, for bulk waves). The exact location of the acoustic source is unimportant for its detection. This makes the acoustic emission technique adequate for crack-propagation studies. Indeed, a great deal of research has been undertaken to investigate the mechanisms of crack growth by

analyzing acoustic signals. Yet, the main effort was directed towards laboratory experiments with appropriately designed, pre-notched specimens [5-11]. The aircraft industry was the first to demonstrate that the acoustic emission generated by fatigue cracks can be detected even in a noisy environment. A few practical applications of monitoring fatigue in aircrafts and other complex structures have been published [12-14].

The present authors have proposed a new nondestructive evaluation technique [15], suggesting that the knowledge of the amplitude distribution of acoustic signals during cyclic stress should enable, by an ordered statistics treatment, the prediction of the actual fatigue lives. A formal relationship was established between the rate of crack-propagation, assumed to occur in discrete steps, and the output acoustic signal amplitude accompanying the propagation step. It was postulated that any statistical distribution of crack-propagation rates gives rise to a one-to-one relationship of distribution of acoustic emission amplitudes. If, from a statistical point of view for fatigue life prediction, an extremal (Frechet) distribution of crack-propagation rates is assumed [16], then the acoustic amplitudes associated with extremal rates have also an extremal distribution [15].

The results of experiments on a 2024-T3 aluminum alloy, undertaken to support the proposed theory, are presented in the Part 1 of this paper. Part 2 [17] reports the results for an Alclad 7075-T6 aluminum alloy.

EXPERIMENTAL PROCEDURE AND RESULTS

The material used in this work was a commercial aluminum alloy 2024-T3. Its chemical composition is given in Table 1 and mechanical properties are given in Table 2. The fracture toughness K_{IC} of the sheet is taken from Ref. 18. Typical grain size and structure are shown in Figure 1. Fatigue specimens were machined from the sheet stock to rectangular shape (16.5 x 200 mm), without any notch or slot. Such specimens are unusual in fatigue experiments. The purpose of this procedure was to perform fatigue tests in the most possible similar conditions to those prevailing in real service. If a crack of any size is to be present in the specimen, it is due to the forming and the machining of the alloy sheet. Initial crack sizes and orientations in the fatigue specimens are therefore entirely randomly distributed. The fatigue tests were conducted in air, at ambient temperature by tension-tension load cycling in a conventional testing machine, at constant load amplitude and low cycles (1-2 Hz), until rupture. The stress ratios were in the vicinity of 0.5. The maximum stresses were chosen to be about 50-70 percent of the yield stress. The tests conditions are given in Table 3, together with the number of cycles to failure. Fractographs were made of the failed specimens, and are shown in Figure 2.

Acoustic emission was monitored by a piezoelectric transducer, resonant in the 150-300 kHz frequency range, coupled to the wedge-action grip of the tensile machine with a viscous resin and held in place with a constant-force clamp. No spurious acoustic emission

whatsoever was detected during the cycling of a specimen gripped at one end only. The acoustic signals were fed into a preamplifier and an amplifier with a total gain setting of 90 dB. The filtering device of the preamplifier was set to a 0.15-0.35 MHz bandpass. After amplification, the signals exceeding 1 volt threshold peak-amplitude were analyzed. The number of ring-downs (counts) of each signal (event) was recorded. The dead-time of the data gathering system was set to 10 msec. The count-rate was evaluated using a reset clock, as counts per second. A distribution analyzer, which performs the counting and the sorting of the acoustic signals (events) according to their number of threshold crossings (equivalent to the peak-amplitude of the signal), enabled the recording to those particular events having the greatest number of crossings (counts) at each preset period of time. These extremal events characterized by an extremal number of counts per event, are produced by the extremal rates of crack propagation in the specimen. The extremal events were recorded every 400 fatigue cycles. The cumulative number of acoustic counts as well as the count-rate were simultaneously chart recorded. Typical acoustic emission behavior is shown in Figure 3. The greatest number of counts per event recorded during each 400 cycles period, as well as the extremal count-rates recorded during the same period of time, are shown in Figure 4.

Following the ordered statistics treatment [19], if the extremal values are indeed extremally distributed, a linear relationship should be obtained on extreme value probability paper. The control curves

obtained by this procedure are shown in Figures 5 and 6. Only the first 9 data of each experiment are used to test the fitting to straight lines. This is done because, according to [15], only the initial crack propagation rates are critical for the fatigue life. The life prediction is therefore possible in an early stage of the cycling process. The variable, appearing on the ordinate in Figures 5 and 6, is the number of counts of the extremal events recorded during each period of 400 cycles. The control curves appear to be very well fitted to straight lines, for all the 8 fatigue tests.

DISCUSSION

Figures 5 and 6 show that the extremal acoustic events generated during 9 periods of 400 fatigue cycles each are extremally distributed. When a straight line,

$$X = U_o + \frac{1}{\alpha} y$$

where X is the extremally distributed variable, is fitted according to the ordered statistics procedure [19] the parameter U_o is the mode of the distribution. The graphically computed values of U_o for each fatigue test are given in Figures 5 and 6. Assuming that the number of counts of a particular acoustic event is linearly related to the peak-amplitude of this event [20], the mode of extremal initial crack propagation rates $(dc/dN)_o$ is obtained through Eqn. 14 in Ref. 15. This mode is used to evaluate the life-time N_F, according to Eqn. 7 of Ref. 15. Doing so, material and equipment parameters are used, given in the Appendix. The initial stress intensity factor ΔK_i and

the initial crack-length were computed for each specimen with its proper conditions of stress and stress-ratio, according to the formulas for plane-stress in thin sheets:

$$(1) \qquad \Delta K_i = \left(\frac{1 - R}{1 + R}\right)^{1/2} \Delta K_{threshold}$$

$$(2) \qquad \Delta K_i = \Delta\sigma\left(\frac{\pi c_i}{2} \sec \frac{\pi c_i}{2w}\right)^{1/2}$$

where $\Delta\sigma$ is the stress-range imposed, c_i the average initial half crack length and $\Delta K_{threshold}$, the ΔK_i value for $R = 0$. The parameters α and M_2 which appear in the stress intensity vs crack-propagation velocity relationship:

$$(3) \qquad \frac{dc}{dN} = M_2(\Delta K)^{\alpha}$$

were calculated from recently published results relative to the same aluminum alloy [21]. These computed values are given in Table 4.

The aim of a statistical theory of extreme-values is to explain observed extremes arising in samples of given sizes or valid for a given period [19]. The essential condition for applying such a theory is that one deals with statistical variants. For the purpose of fatigue-life prediction, only the highest crack-propagation rates are significant. Furthermore, the assumption that these rates, because of their extremal character, are extremally (Frechet) distributed, is the basic idea of Freudenthal's theory [16,22].

It is well established that the crack-propagation during fatigue processes occurs in discrete steps. The formal connection of the energy released at each step by the propagation of a crack at a certain velocity (dc/dN) with the peak-amplitude V_i of the acoustic emission signal accompanying the step propagation has been derived in Ref. 15:

$$(4) \qquad V_i \cong a\ b\ G \left(\frac{dc}{dN}\right)^{1/\alpha+1/2}$$

where a is a transducer constant, b a material constant and G the gain of the electronics. It was assumed [15] that the right and left hand parts of Eqn. (4) were directly proportional, but not equal. In order to make practical correlations, one has to know what is the fraction β of the elastic stored energy released during crack-propagation which is converted into kinetic energy to give use to a stress-wave.

$$(5) \qquad V_i = \beta\ b\ G\left(\frac{dc}{dN}\right)^{1/\alpha+1/2}$$

According to a model for estimating the signal from an acoustic emission source by means of appropriate transfer functions [23] a step stress function generates an oscillating acoustic emission signal with a peak-acoustic emission amplitude. The fraction of energy transmitted by the transducer to the amplification chain appears to be of the order of magnitude of 10^{-10} V μbar^{-1}, much less than the conventional sensitivity factor of commercial transducers. In Eqn. (5),

the parameter a has been included in β, which is now the numerical value of the transducer transfer function. In the present work, the values of β, the apparent transducer sensitivity, were arbitrarily computed for the three last fatigue experiments, from the known actual fatigue-lives, thus obtaining a value of 10^{-8} ($\pm 0.1 \times 10^{-8}$) Ref. $IV_{\mu bar}^{-1}$. This value was then introduced as a transducer transfer function to predict the number of cycles to failure for the 5 first experiments, using the computed modes U_o obtained after only 9 periods of 400 cycles. These fatigue lives, predicted at a probability of 63 percent [19], are presented in Table 5.

The results of the present experiment show the peak-acoustic emission amplitudes produced during fatigue tests are indeed extreme values. They are extremally distributed according to the Second Asymptotic Distribution of largest values due to Frechet [19]. This is proven by the satisfactory fitting of the extremal counts, obtained from the acoustic emission data, to straight-lines on extremal probability paper (Figures 5 and 6). Considering each extremal event to be equivalent to an extremal crack-propagation rate, itself associated to a minimum expected life-time N_F (through Eqn. (5) in Ref. [15]), the distribution of the possible fatigue-lives is the Weibull distribution of smallest values. The prediction of these fatigue-lives is then determined through Eqn. (7) in Ref. [15], and is shown in Table 5. The agreement with the actual fatigue lives is satisfactory. However, the entire procedure has to be improved. The fact that the present acoustic emission system did not allow the direct reading of peak-

amplitudes by impairs somehow the validity of the relationship between peak amplitudes, as evaluated from ringdown counts through an assumed linear dependence, and crack-propagation rates. Moreover, it is not clear what is the most appropriate "sampling" procedure (every 400 fatigue cycles). The present experiments were performed in the state of plane-stress in their sheets. The influence of plane-strain has to be investigated, as well as the grain-size and the mechanical properties of the material.

A surprising feature of the experimental results is the fact that no abrupt increase in the cumulative counts towards the end of the fatigue tests was noticed (see Figure 3). This is contradictory to other reported experiments on monitoring fatigue crack-growth by acoustic emission techniques [5,6-8]. This could be due to the fact that the present experiments employed un-notched specimens, leaving stress-concentration to be at random locations rather than at the notch tip. It is, therefore, recommended that experiments which are guided towards the applicability of acoustic emission technique to non-destructive evaluation, should be performed on un-notched specimens, which are more representative of real structures.

The results of the present experiments do strongly support the phenomenological theory developed in Ref. [15]. The knowledge of the distribution function of crack propagation rates during fatigue is essential for design and maintenance. Such knowledge can be obtained in a nondestructive manner during service under fatigue conditions by analyzing the distribution of amplitudes of acoustic emission signals

emitted during cyclic stress, as shown in the present investigation. The procedure appears to be an original and promising nondestructive method of predicting fatigue life.

CONCLUSIONS

A formal relationship between acoustic emission amplitudes and initial fatigue crack-propagation rates during cyclic stress has been proven to exist, for an aluminum 2024-T3 alloy. Both quantities are extremally distributed and can be treated by ordered statistics. Such a treatment affords the early prediction of fatigue-lives during the first stages of the fatigue process, which are in fair agreement with the actual lives. The analysis of the amplitude distribution of the acoustic signals emitted during cyclic stress provides a promising nondestructive method of predicting fatigue life.

ACKNOWLEDGMENT

This study has been performed in the NDT Laboratory of the Materials Engineering Department, Ben Gurion University, Beer Sheva, Israel.

This work was supported by the Materials and Molecular Research Division of the U. S. Department of Energy under contract No. W-7405-ENG-48.

Table 1. 2024-T3. Chemical composition weight percent.

	Si	Fe	Cu	Mn	Mg	Cr	Ti	Al
7072 cladding	0.45	0.25	4.10	0.45	1.65	0.10	0.05	Remainder

Table 2. 2024-T3. Mechanical properties.

Thickness [mm]	Yield Stress [kg/mm^2]	Ultimate Stress [kg/mm^2]	Fracture Toughness [ksi in.]
1.65	28.8	49.2	35.0 [18]

Table 3. 2024-T3 - Fatigue Tests Conditions

No. of Spec.	σ_{max} [kg/mm^2]	σ_{min} [kg/mm^2]	Stress Ratio	Cycling Frequency [Hz]	Number of Cycles to Failure
1.	20.3	10.0	0.49	1.8	25015
2.	19.7	10.0	0.51	1.78	27827
3.	14.2	4.9	0.34	1.0	6994
4.	14.8	5.8	0.39	1.0	12523
5.	16.7	7.6	0.45	1.0	2022
6.	16.7	7.9	0.47	1.0	2318
7.	15.6	7.4	0.48	1.25	12991
8.	15.8	7.6	0.48	1.12	10649

Table 4. 2024-T3. Fatigue parameters.

Spec. No.	Initial Stress Intensity Factor Δk_i [Ksi $in.^{1/2}$]	Initial Half Crack Length [cm]	Stress Range $\Delta\sigma$ (kg/cm^2)	Stress Rates R
1.	2.04	1.57×10^{-2}	1.03×10^{3}	0.493
2.	2.00	1.70×10^{-2}	0.97×10^{3}	0.508
3.	2.46	2.73×10^{-2}	0.935×10^{3}	0.340
4.	2.32	2.62×10^{-2}	0.904×10^{3}	0.388
5.	2.14	2.22×10^{-2}	0.912×10^{3}	0.455
6.	2.09	2.27×10^{-2}	0.882×10^{3}	0.473
7.	2.09	2.60×10^{-2}	0.818×10^{3}	0.476
8.	2.07	2.57×10^{-2}	0.822×10^{3}	0.481

Table 5. 2024-T3. Predicted fatigue-lives

Spec. No.	Actual Fatigue Life	Predicted Fatigue Life	Cycle of Prediction
1.	25015	21605	3600
2.	27827	32615	3600
3.	6994	4066	3600
4.	92523	9794	3600
5.	7022	9456	3600
6.	7318		
7.	12991		
8.	10649		

APPENDIX: 2024-T3 ALLOY

Experimental values for the variables used in Eqs. (2), (5), (6) and (14) of Ref. [15] for the present experiment are given below. Some of them were taken from the most recent literature.

material's density	ρ - [g-cm^{-3}]	2.7
Young's modulus	E - [dynes cm^{-2}]	7.1×10^{11}
specimen width	W - [cm]	2.05
material's thickness	B_S - [cm]	0.165
surface wave velocity	v - [cm sec^{-1}]	2.77×10^{5}
Fracture toughness	K_{IC} [Ksi in.$^{1/2}$]	35
Initial stress intensity factor	K_i [ksi in.$^{1/2}$]	3.5* for R=0
α		3*
K_2	in.$^{\frac{3\alpha+2}{2}}$ klb$^{-\alpha}$ sec^{-1}	10^{-9}
γ		4.5**
Frequency of cycling	[Hz]	1-1.8
Transducer sensitivity	gBc [Ref. μbar^{-1}	1.778×10^{-4}
Gain of the electronic system	G	3.16×10^{4}

*These values were calculated from recently published results on the same alloy [21].

**Taken from [16].

REFERENCES

[1] D. V. Nelson, Review of fatigue crack growth prediction methods, Exp. Mechanics 17, 41 (1977).

[2] J. Schijve, Four lectures on fatigue crack growth, Eng. Fracture Mech. 11, 167 (1979).

[3] W. Shutz, The prediction of fatigue life in the crack initiation and propagation stages—a state of the art survey, Eng. Fracture Mech. 11, 405 (1979).

[4] K. H. Schwalbe, Comparison of several fatigue crack propagation laws with experimental results, Eng. Fracture Mech. 6, 325 (1974).

[5] H. L. Dunegan, D. O. Harris and A. J. Tetelman, Detection of fatigue crack growth by acoustic emission techniques, Mat. Evaluation 17, 221 (1970).

[6] C. E. Hartbower, C. F. Morais, W. G. Reuter and P. P. Crimmins, Acoustic emission from low-cycle high stress intensity fatigue, Eng. Fracture Mech. 5, 765 (1973).

[7] T. M. Morton, R. M. Harrington and J. G. Bjetelich, Acoustic emission of fatigue crack growth, Eng. Fracture Mech. 5, 691 (1973).

[8] D. O. Harris and H. L. Dunegan, Continuous monitoring of fatigue crack growth by acoustic emission techniques, Exp. Mech. 14, 71 (1974).

[9] Y. Krampfner, A. Kawamoto, K. Ozo and A. T. Green, Acoustic emission characteristics of Copper alloys under low-cycle fatigue conditions, NASA Report CR-134766 (April (1975).

[10] A. C. E. Sinclair, D. C. Connors and C. L. Formby, Acoustic emission during fatigue crack growth in steel, Mat. Sci. Eng. 28, 263 (1978).

[11] T. C. Lindley, I. G. Palmer and C. E. Richards, Acoustic emission monitoring of fatigue crack growth, Mat. Sci. Eng. 32, 1 (1978).

[12] Y. Nakamura, Acoustic emission monitoring system for detection of cracks in a complex structure, Mat. Evaluation 29, 8 (1971).

[13] C. D. Bailey and W. M. Pless, Acoustic emission--monitoring fatigue cracks in aircraft structure. Instrument Society of America 22nd Intern. Instrumentation Symp., San Diego, CA (May 1976).

[14] C. D. Bailey, J. M. Hamilton and W. M. Pless, AE monitoring of rapid crack growth in a production size wing fatigue test article, NDT Intern. 10, 298 (1976).

[15] J. Baram and M. Rosen, Fatigue life prediction by distribution analysis of acoustic emission signals, Mat. Sci. Eng. 41, 9 (1980).

[16] A. M. Freudanthal, Reliability of reactors components and systems subject to fatigue and creep, Nucl. Eng. Design 28, 196 (1974).

[17] [PART II]

[18] J. G. Kaufman, R. L. Moore and P. E. Schilling. Fracture toughness of structural aluminum alloys, Eng. Fracture Mech. 2, 197 (1971).

[19] E. J. Gimbel, Statistical theory of extreme values and some practical applications, National Bureau of Standards (U.S.) Monograph 33, 1954.

[20] E. Esmail and I. Grabec, Application of a signal recovery technique to acoustic emission analysis, Ultrasonics 16, 87 (1978).

[21] T. L. Mackay, Fatigue crack propagation rate at low Δk of two aluminum sheet alloys, 2024-T3 and 7075-T6, Eng. Fracture Mech. 11, 753 (1979).

[22] A. M. Freudenthal, New aspects of fatigue and fracture mechanics. Technical report No. 16 (December 1973). Office of Naval Research, Airforce Materials Laboratory.

[23] L. Bolin, A model for estimating the signal from a acoustic emission source, Ultrasonics 17, 67 (1979).

FIGURE CAPTIONS

Figure 1. 2024-T3. Typical grain size and structure (L-cut) Keller's reagent. Magnification: 100.

Figure 2. 2024-T3. Fractographs (Scanning Electron Microscope).
(a) Magnification: 1300
(b) Magnification: 2400
Striations are clearly visible as well as micro-cracks.

Figure 3. 2024-T3. Acoustic emission behavior
count rate vs fatigue cycle
cumulative counts vs fatigue cycle.

Figure 4. 2024-T3. Extremal count rates and extremal counts per event vs fatigue cycle.

Figure 5. Extremal statistics control curves. Spec. Nos. 1-4.

Figure 6. Extremal statistics control curves. Spec. Nos. 5-8.

Fig. 1

XBB 804-5342

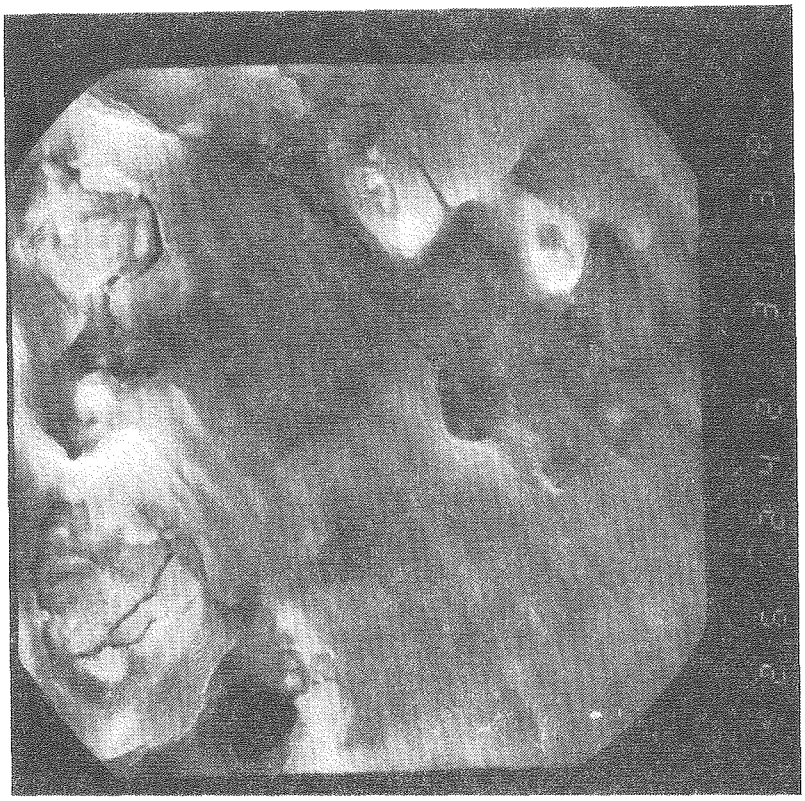

XBB 804-5344

Fig. 2b

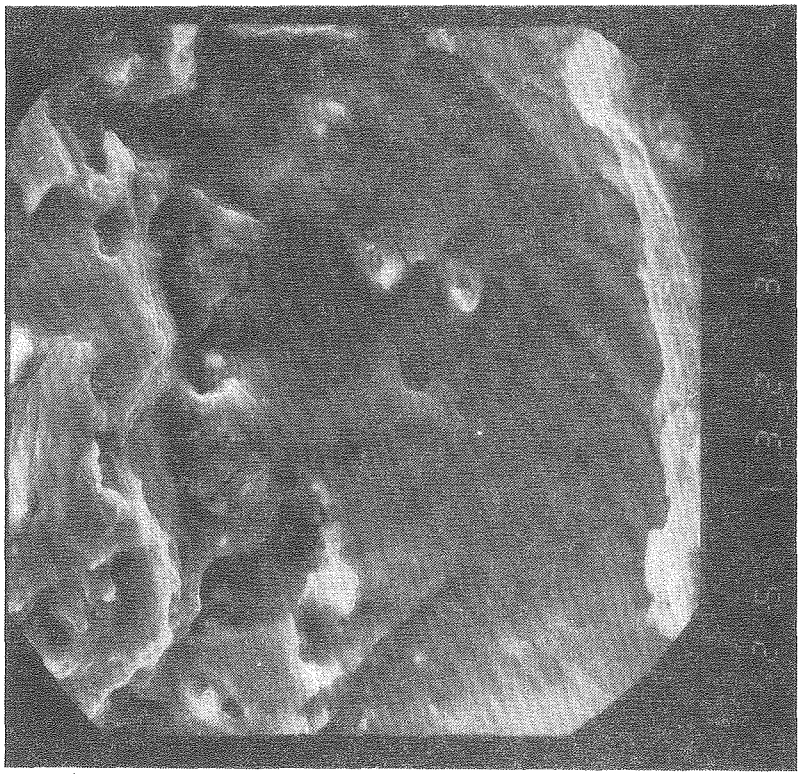

XBB 804-5343

Fig. 2a

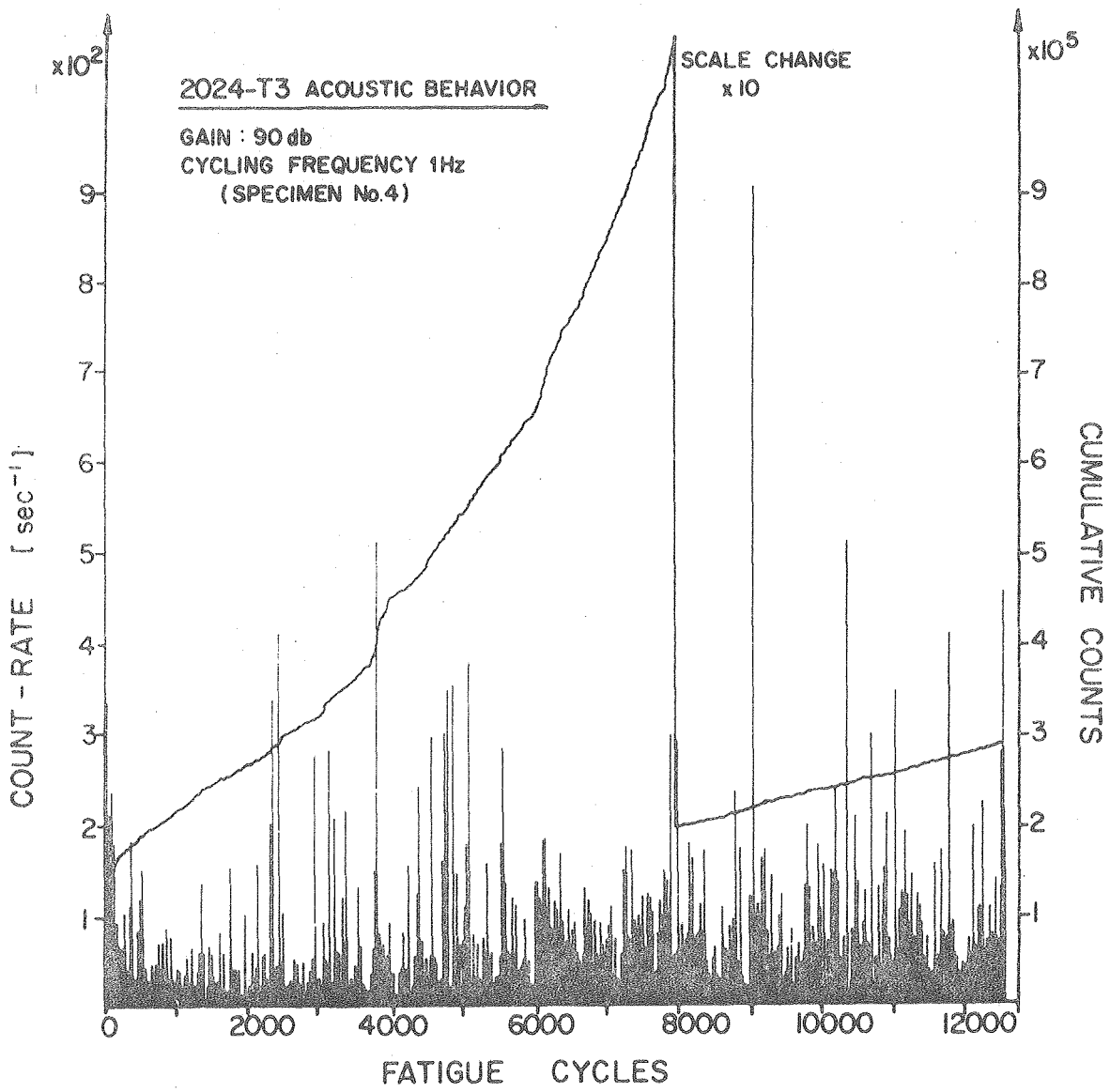

XBL 805-9490

Fig. 3

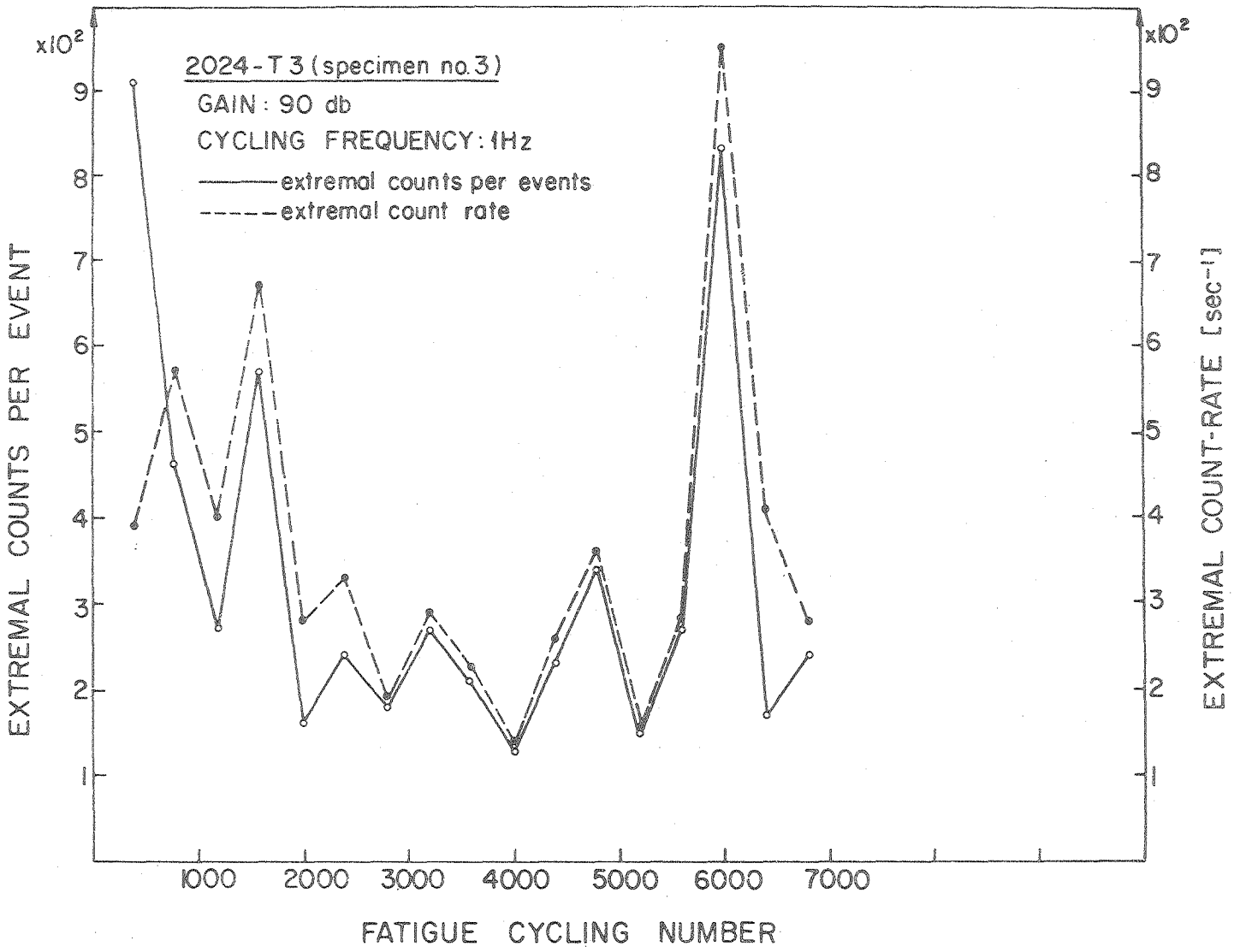

XBL 805-9485

Fig. 4

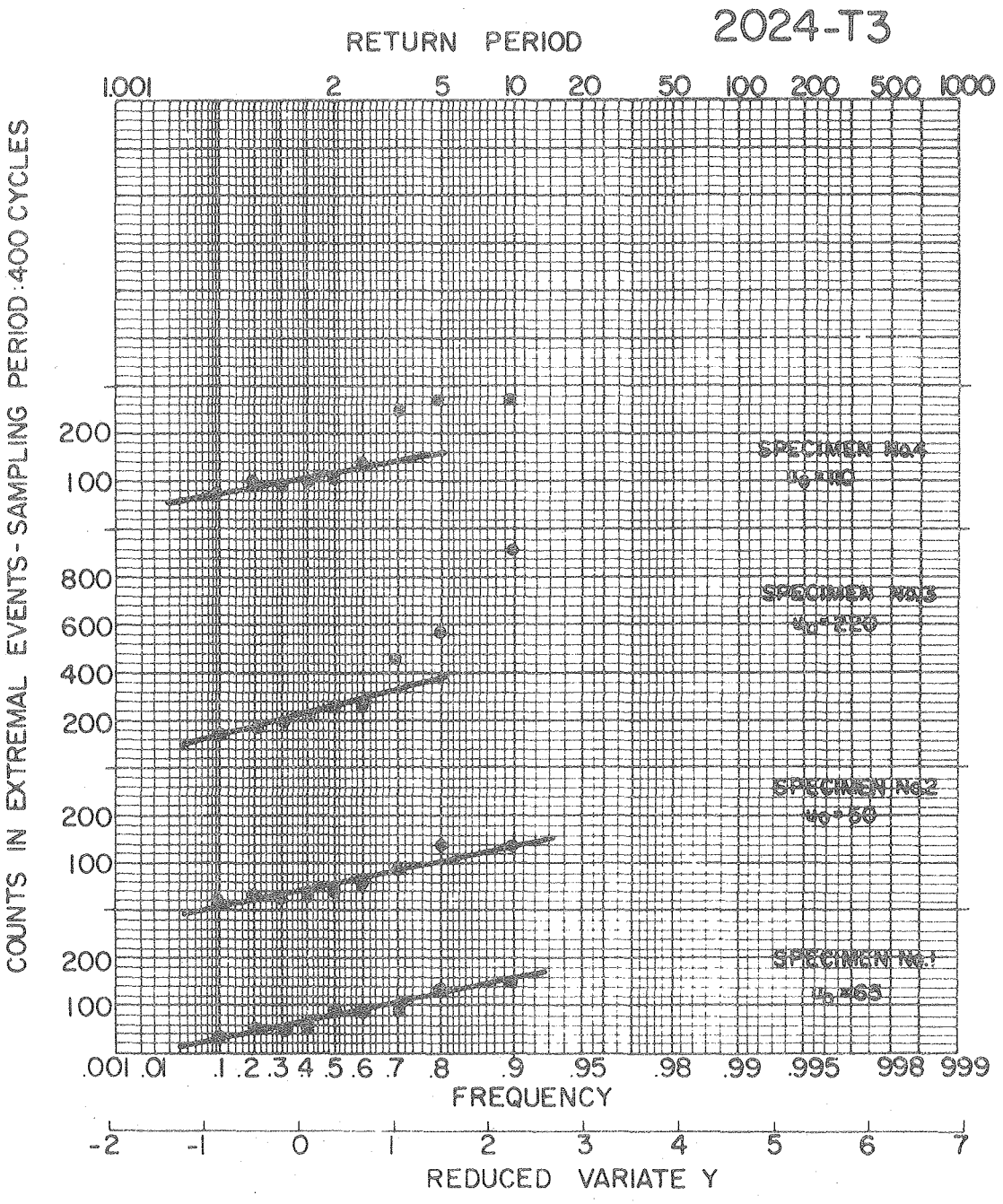

XBL 805-9486

Fig. 5

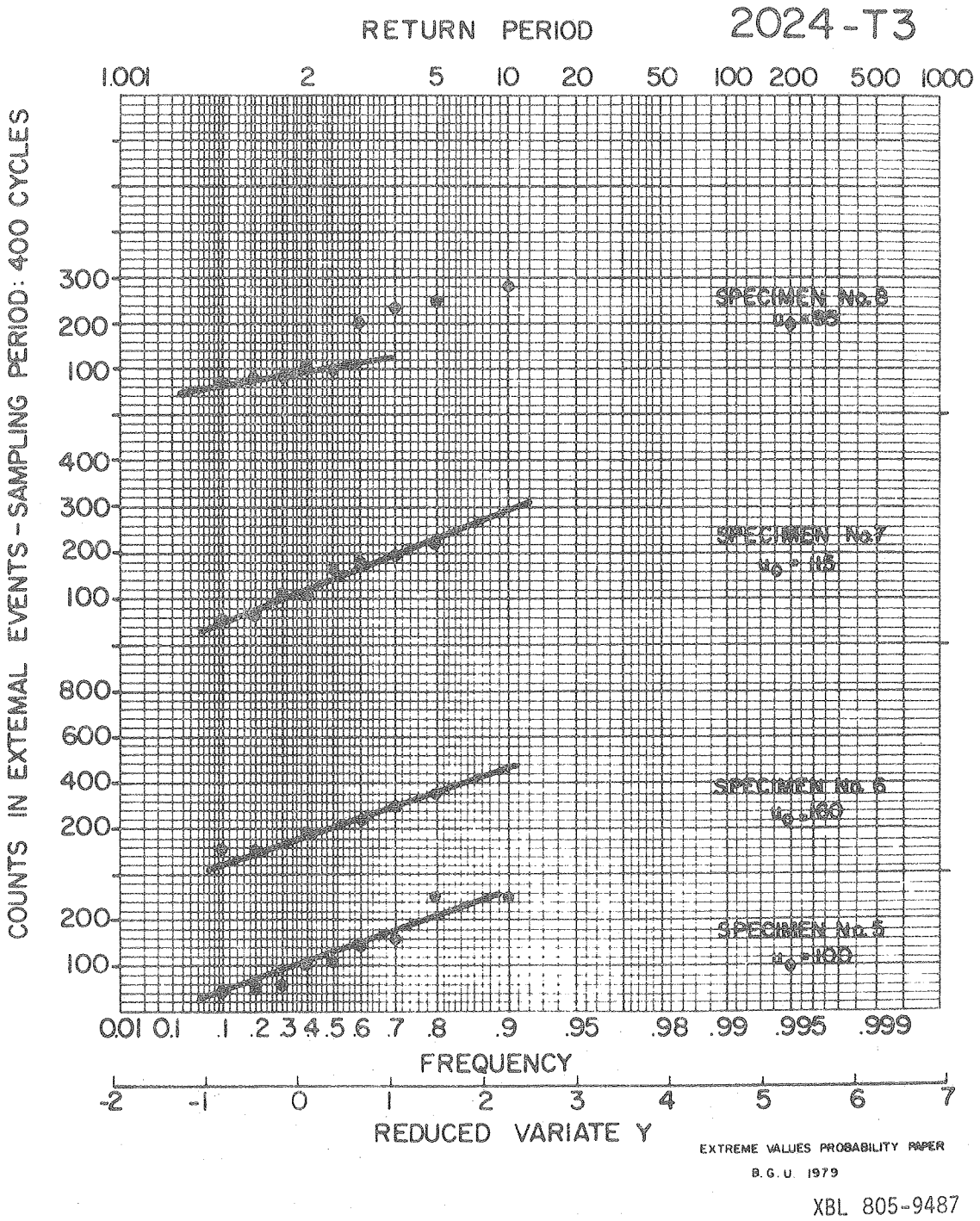
2024-T3
RETURN PERIOD
1.001
2
5
10
20
50
100
200
500
1000
COUNTS IN EXTEMAL EVENTS - SAMPLING PERIOD: 400 CYCLES
300
200
100
400
300
200
100
800
600
400
200
200
100
SPECIMEN No.8
SPECIMEN No.7
SPECIMEN No.6
SPECIMEN No.5
0.01 0.1 .1 .2 3 4 .5 6 .7 .8 .9 .95 .98 .99 .995 .999
FREQUENCY
-2 -1 0 1 2 3 4 5 6 7
REDUCED VARIATE Y
EXTREME VALUES PROBABILITY PAPER
B.G.U. 1979
XBL 805-9487

Fig. 6

PREDICTION OF LOW-CYCLE FATIGUE LIFE BY ACOUSTIC EMISSION PART 2: ALCLAD 7075-T6/ALUMINUM ALLOY

J. Baram
Materials Engineering Department
Ben Gurion University of the Negev
Beer Sheva, Israel

and

M. Rosen*
Materials and Molecular Research Division
Lawrence Berkeley Laboratory
University of California
Berkeley, California 94720
U.S.A.

SUMMARY

Low cycle high stress fatigue tests were conducted by tension-compression on an Alclad 7075-T6 aluminum sheet alloy, until rupture. Initial crack sizes and orientations in the fatigue specimens were randomly distributed. Acoustic emission was continuously monitored during the tests. Extremal peak-amplitudes, equivalent to external crack-propagation rates, are shown to be extremally Weibull distributed. The prediction of the number of cycles left until failure is made possible, using an ordered statistics treatment and an experimental equipment parameter obtained in previous experiments (Part 1). The predicted life-times are in good agreement with the actual

---

*On leave from the Materials Engineering Department, Ben Gurion University, Beer-Sheva, Isreal.

fatigue lives. The amplitude distribution analysis of the acoustic signals emitted during cyclic stress has been proven to be a feasible nondestructive method of predicting fatigue life.

INTRODUCTION

In Part 1 [1], an ordered statistics treatment was applied to acoustic emission data recorded during recorded low-cycle fatigue experiments on a commercial 2024-T3 aluminum alloy. It was postulated that the statistical behavior of the acoustic emission amplitudes follows the statistical behavior of crack propagation rates during fatigue cycling. The formal relationship between emission amplitudes and propagation-rates which was used, has been developed in [2]. Prediction of the fatigue lives, as early as after 3600 elapsed fatigue cycles, accounting for 20-50 percent of the actual fatigue lives for each experiment, was possible, with a fair agreement to these actual lives. In Part 2, experimental results are reported for a Alclad 7075-T6 aluminum sheet alloy.

EXPERIMENTAL PROCEDURE AND RESULTS

The chemical composition of the material is given in Table 1, the mechanical properties in Table 2. Typical grain-size and structure is shown in Fig. 1. Fatigue specimens were machined from the commercial sheet stock to rectangular shape (20 x 200 mm), without notches or slots. The reason for this procedure is explained in Part 1. The

fatigue tests were conducted in air, at room temperature, by tension-tension load cycling at constant load amplitude and low cycles (1 Hz), until rupture. The stress-ratios were in the vicinity of 0.5. The maximum stresses were chosen to be about 75-85 percent of the yield stress. The test conditions are given in Table 3, together with the number of cycles to failure. Fractographs of failed specimens are shown in Fig. 2. The acoustic emission monitoring and data gathering system has been extensively described in Ref. [1]. Extremal events were recorded every 150-200 fatigue cycles. Typical acoustic emission behavior is shown in Figs. 3 and 4. Table 4 gives the experimental results. Specimens 1-4 were monitored every 200 cycles, beginning from the cycle 200. Specimens 5-10 were monitored every 150 cycles, beginning from the cycle 150. The control curves obtained by the ordered statistics treatment [4] by using only the first 9 data points of each experiment, are shown in Figs. 5 and 6. As was mentioned in Part 1 [1], the variable appearing on the ordinate in these figures is the number of counts of the external events recorded during each period of 150 or 200 cycles. The control curves appear again to be well fitted to straight-lines for the most of the 10 fatigue tests.

The graphically computed values of u_o, the extreme value distribution mode, are given in Figs. 5 and 6. The evaluation of the predicted life-times was done according to Eq. 7 of Ref. [2]. The material and equipment parameters used are given in the Appendix. Initial stress-intensity factors ΔK_i, and initial crack-lengths were

calculated for each specimen with its proper conditions of stress and stress-ratio, as explained in [1]. The parameters α and M_2 were calculated from published results for the same aluminum alloy [5]. All these computed values are given in Table 5. The transducer transfer function (β in Eq. [5] of Ref. [1]) was taken as 10^{-8} ($\pm 0.1 \times 10^{-8}$), Ref. 1V μbar^{-1}, which is the value introduced in Ref. [1], according to the 2024-T3 aluminum results. Doing so, it is assumed that the frequency content of acoustic signals during crack-propagation in the 2024 alloy is the same as during the crack-propagation in a 7075 alloy.

The fatigue lives for the 10 specimens of 7075-T6, predicted at a probability of 63 percent [4], are presented in Table 6.

DISCUSSION

The predicted fatigue lives are in fair agreement with the actual fatigue lives. The prediction was made possible after a relatively long time elapsed, compared to the short actual lives. These short lives are due to the high levels of stress and stress ratios. The sampling sequence (every 200 at 150 cycles) is probably not adequate, and extreme events should have been recorded at shorter intervals. The discrepancy of the predicted fatigue lives compared to the actual lives is higher, the shorter the actual fatigue life (Spec. No. 4, 8 and 10). In contrast to the results obtained for the 2024-T3 alloy, the actual fatigue lives of the Alclad 7075-T6 alloy are inversely proportional to the stress-ratios. The fatigue damage is propagating

faster in the 7075 alloy than in 2024. This is clearly demonstrated by the denser spacing of the striations (compare Figs. 2 in the two parts of this report) on the scanning electron micrographs, at the same magnification.

This study, in both parts, was conducted in order to provide experimental support to the phenomenological theory developed in Ref. [2]. The results of this feasibility study, for both materials under investigation, are promising. In this context, the fact that the numerical value experimentally obtained for one alloy was adequate for the other alloy is encouraging.

CONCLUSIONS

The statistical distribution of external amplitudes of acoustic emission signals emitted during cyclic stress has been shown to be associated with the distribution of external crack propagation rates in the early stages of the fatigue process. The knowledge of the initial crack propagation rates distribution enables the prediction of the number of cycles left until failure, which is essential to prevent the catastrophic damage of fatigued structures. An equipment parameter, the acoustic emission transducer transfer function, which was obtained in experiments on a 2024-T3 alloy reported in [4] was used to predict the fatigue lives of 10 specimens of an Alclad 7075-T6 alloy, in good agreement with the actual lives. The acoustic emission technique provides an original nondestructive method to assess the fatigue behavior of commercial 2024 and 7075 aluminum sheet alloys.

ACKNOWLEDGMENTS

This study has been performed in the NDT Laboratory of the Materials Engineering Department of Ben Gurion University, Beer-Sheva. The able experimental assistance of Miss R. Tottman is highly appreciated.

This work was supported by the Materials and Molecular Research Division of the U. S. Department of Energy under contract No. W-7405-ENG-48.

REFERENCES

[1] J. Baram and M. Rosen. Prediction of low-cycle fatigue life of Aluminum sheet alloys by acoustic emission. Part 1: 2024-T3 alloy. Eng. Fracture Mech. (submitted).

[2] J. Baram and M. Rosen. Fatigue life prediction by distribution analysis of acoustic emission signals. Mat. Sci. Eng., 41 25 (1979).

[3] J. G. Kaufman, R. L. Moore, and P. E. Schilling. Fracture toughness of structural aluminum alloys. Eng. Fracture Mech., 2, 197 (1971).

[4] E. J. Gumbel. Statistical theory of extreme values and some practical applications. National Bureau of Standards (U.S.) Monograph 33 (1954).

[5] T. L. Mackay. Fatigue crack propagation rate at low ΔK of two aluminum sheet alloys, 2024-T3 and 7075-T6. Eng. Fracture Mech., 11, 753 (1979).

Table 1. Chemical Composition

	Si	Fe	Cu	Mn	Mg	Cu	Zn	Al
7072 cladding	0.35	0.30	0.20	0.10	0.20	0.05	0.85	Remainder
7075-T6	0.40	0.80	2.10	0.07	2.45	0.20	7.00	Remainder

Table 2. Mechanical properties - Alclad 7075-T6

Thickness [mm]	Field Stress [kg/mm^2]	Ultimate Stress [kg/mm^2]	Fracture Toughness [psi u]	
2.0	45.6	55.3	60	[3]

Table 3. Alclad 7075-T6 - Fatigue Tests Conditions

No. of Spec.	σ_{max} (kg/mm^2)	σ_{min} (kg/mm^2)	Stress Ratio	Cycling Frequency (Hz)	Number of Cycles to Failure
3.	29.0	12.75	0.66	1.0	3551
2.	28.25	11.00	0.39	1.0	4164
3.	27.50	11.00	0.40	1.0	4364
4.	32.50	16.25	0.50	1.0	2508
5.	28.00	11.75	0.42	1.0	4070
6.	29.25	13.25	0.45	1.0	3567
7.	27.75	11.75	0.42	1.0	3917
8.	32.50	16.50	0.51	1.0	1698
9.	27.50	11.50	0.42	1.0	3979
10.	28.50	13.00	0.46	1.0	2848

Table 4. Counts of Extremal Acoustic Events - Alclad 7075-T6

Specimen No.	Cycle No.										
	1000	1400	1800	2200	2600	3000	3400	3800	4000	4200	4400
1	270	270	1500	3300	2800	3500	6400	FAILURE			
2	800	2000	1200	1100	2300	2300	1700	1300	800	FAILURE	
3	900	2200	1800	1400	1400	4600	2600	1400	1000	900	FAILURE
4	800	800	1300	1200	FAILURE						
5	2000	900	800	3200	1300	800	2800	1000	700	FAILURE	
6	600	600	1000	500	500	800	900	FAILURE			
7	800	1800	400	600	900	400	700	400	FAILURE		
8	200	300	FAILURE								
9	1500	600	1800	300	700	500	4900	5100	4800	FAILURE	
10	600	1000	700	800	100	FAILURE					

Table 5. ALCLAD 7075-T6 - Fatigue Parameters

Spec. No.	Initial Stress Intensity Factor Δk_i [ksi cm]	Initial Half Crack Length (cm)	Stress Range Δ (kg/cm^2)	Stress Rates R
1.	1.75	$4.62.10^{-3}$	$1\ 72.10^3$	0.440
2.	1.86	$4.63.10^{-3}$	$1.73.10^3$	0.389
3.	1.83	$4.94.10^{-3}$	$1.65.10^3$	0.400
4.	1.62	$3.96.10^{-3}$	$1.62.10^3$	0.500
5.	1.79	$4.85.10^{-3}$	$1.62.10^3$	0.420
6.	1.72	$4.61.10^{-3}$	$1.60.10^3$	0.453
7.	1.78	$4.96.10^{-3}$	$1.60.10^3$	0.423
8.	1.60	$4.00.10^{-3}$	$1.60.10^3$	0.508
9.	1.79	$5.03.10^{-3}$	$1.60.10^3$	0.418
10.	1.71	$4.88.10^{-3}$	$1.55.10^3$	0.456

Table 6. ALCLAD 7075-T6 - Predicted Fatigue-Lives

Spec. No.	Actual Fatigue Life	Predicted Fatigue Life	Cycle of Prediction
1.	3551	2747	2200
2.	4164	4145	2000
3.	4346	3455	1800
4.	2508	3554	2000
5.	4070	4122	1500
6.	3567	3726	1500
7.	3917	4212	1350
8.	1698	4900	1350
9.	3979	4054	1350
10.	2848	5560	1350

APPENDIX

ALCLAD 7075-T6 ALLOY

Experimental values for the variable used in Equs. 2, 5, 6, and 14 of Ref. [15] for the present experiment are given below.

Specimen width w - [cm]: 2.00

Material's Thickness B_5 - [cm]: 2.00

Fracture toughness K_{IC} - [Ksi $\sqrt{cm}$] 60

Initial stress intensity factor k_i - [ksi $\sqrt{cm}$]: 2.8* for R = 0

α : 4*

M_2 $[\text{in } \frac{3\alpha x2}{2} \; k_{\text{pound}}^{-\alpha_\vartheta \; -1}]$: $3.5.10^{-8}$*

Frequency of cycling $[H_z]$: 1.0

Gain of the electronics G: $3.16.10^4$

---

*Calculated from results published in Ref. [21] in Part 1.

**Taken from Ref. [10] in Part 1.

CAPTION TO FIGURES

Figure 1. Alclad 7075-T6 - Typical grain size and structure (L-Cu4)
Keller's reagent
Magnification: 100

Figure 2. Alclad 7075-T6 fractographs (Scanning Electron Microscope
a) Magnification: 1000
b) Magnification: 2000
Striations are clearly visible, as well as microcracks
μμaulding apparent on b)

Figure 3. Alclad 7075-T6 - Acoustic emission behavior
Count-rate vs. fatigue cycle
Cummulative counts vs. fatigue cycle

Figure 4. Alclad 7075-T6 - Extremal count-rates and extremal counts per event vs. fatigue cycle

Figure 5. Extremal statistics control curves - Spec. nos. 1-5

Figure 6. Extremal statistics control curves - Spec. nos. 6-10

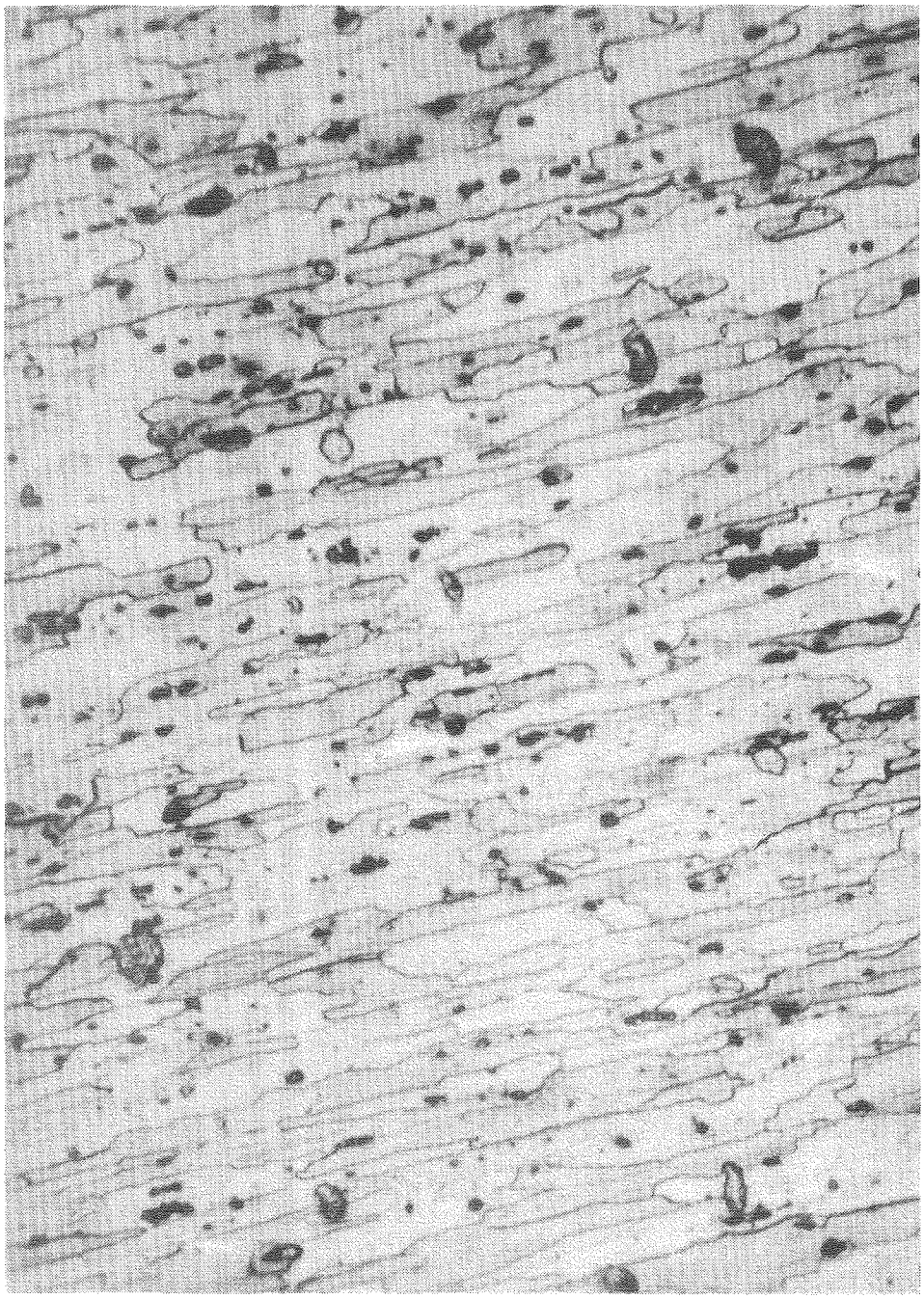

XBB 804-5345

Fig. 1

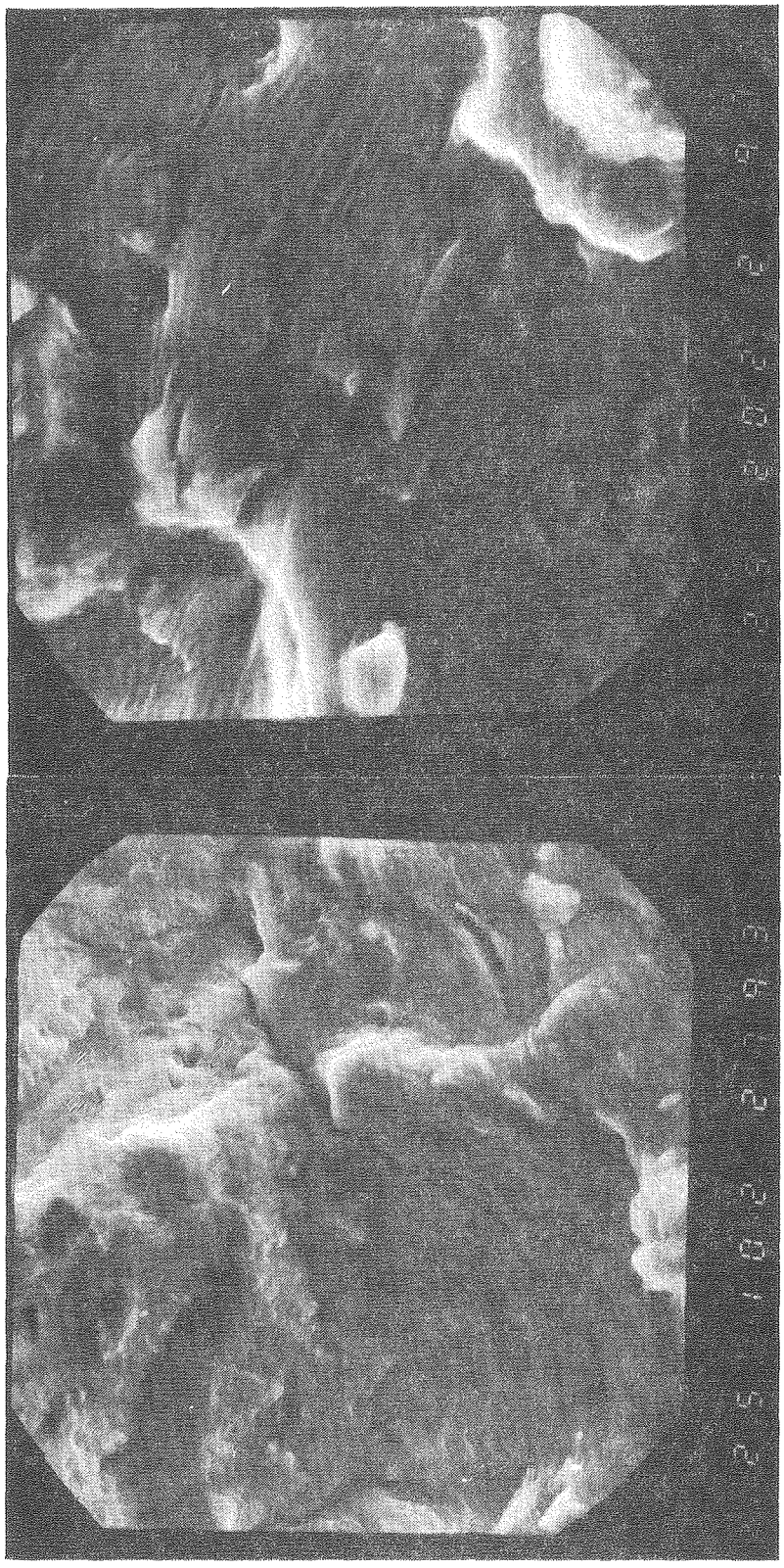

XBB 804-5347

Fig. 2b

XBB 804-5346

Fig. 2a

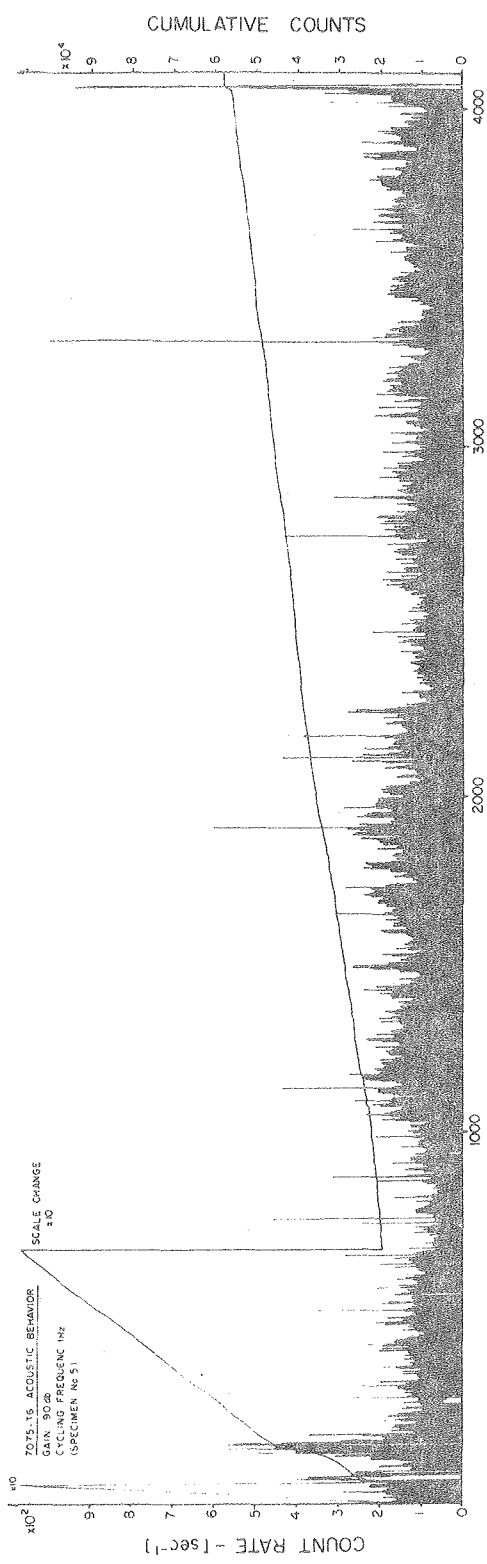

XBL 805-9482

Fig. 3

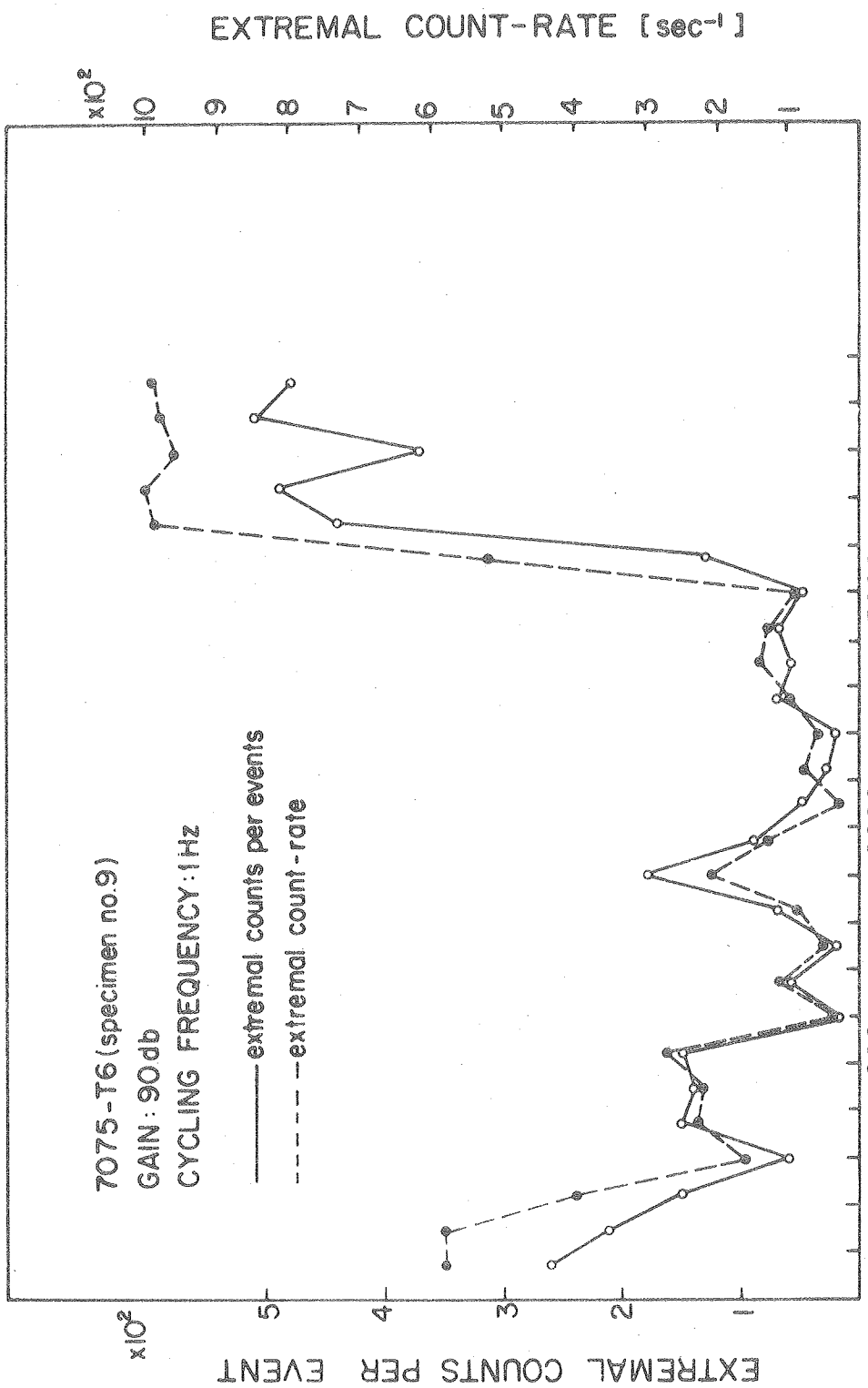

XBL 805-9481

Fig. 4

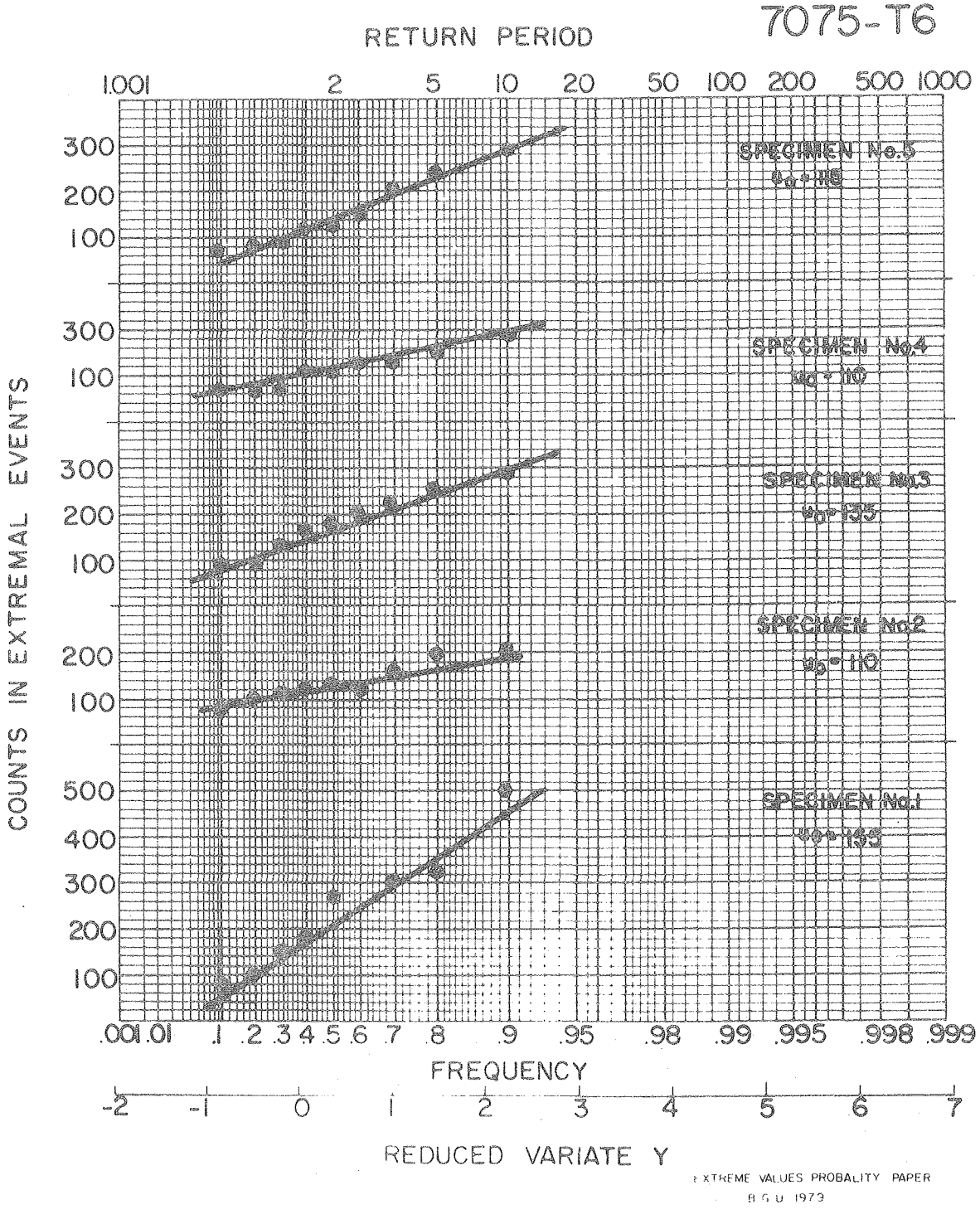

XBL 805-9483

Fig. 5

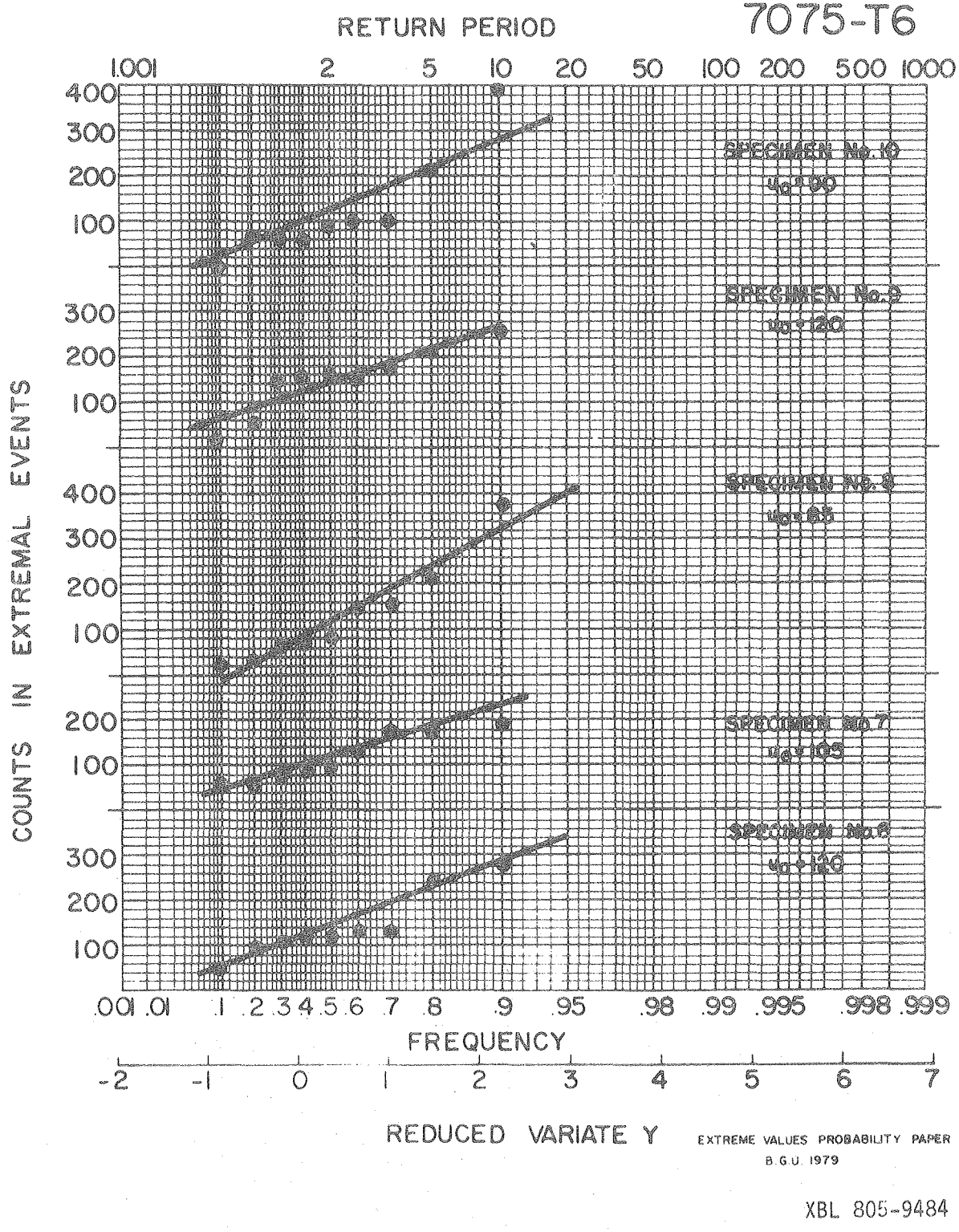

XBL 805-9484

Fig. 6